Ali Nikkhoo · Ali Farazandeh · Mohsen Ebrahimzadeh Hassanabadi · Stefano Mariani

Simplified modeling of beam vibrations induced by a moving mass by regression analysis

Received: 3 October 2014 / Revised: 5 December 2014 / Published online: 31 January 2015

1 Introduction

Two typical types of modeling standpoints employed to assess the dynamic behavior of a beam structure traversed by a moving load are the *moving force* and the *moving mass*. In this regard, the governing constraint equation of moving load/substructure contact force is assigned. Formulating the problem according to *moving force*, the inertial effects of the traversing inertial load on the substructure are ignored. To compensate for this deficiency, the *moving mass* should be adopted. Transverse acceleration of the beam beneath the traveling load in any time should be computed to reveal the load/structure interactions; wherein, a significant complexity is added to the numerical simulation.

A voluminous literature on the vibration of a structure exposed to the excitation by a moving load could be found. The early studies have been generally devised according to the moving force problems [1–5]. However, several articles have been published emphasizing the simulation and significance of the load/structure inertial interaction. Akin and Mofid [6] studied the dynamic behavior of an Euler–Bernoulli beam with various boundary conditions subjected to a moving mass to assess the effects of mass inertia in the modeling. They indicated that the critical dynamic response of the system is occurring at the high levels of mass velocity and weight. Rao [7] accounted for the terms relevant to centripetal and Coriolis accelerations of the inertial

A. Nikkhoo (✉) · A. Farazandeh
Department of Civil Engineering, University of Science and Culture (USC), P. O. Box 13145-871, Tehran, Iran
E-mail: nikkhoo@usc.ac.ir
Tel.: +98-21-44252045

M. Ebrahimzadeh Hassanabadi
Department of Structural Engineering, Building and Housing Research Center (BHRC), Tehran, Iran

S. Mariani
Department of Civil and Environmental Engineering, Politecnico di Milano, Piazza L. da Vinci 32, 20133 Milan, Italy

load on the dynamics of an Euler–Bernoulli beam with simple end conditions. Moreover, Michaltsos and Kounadis [8] investigated the influences due to centripetal and Coriolis forces on the dynamic response of light bridges under moving loads. Ichikawa et al. [9] have considered the inertial effects of the traveling mass in the formulation of a multi-span beam. The results confirmed the importance of inertial effects in evaluating the dynamic response of the structure, especially for the moving masses with high weight and velocity. Nikkhoo et al. [10] identified a *critical velocity* for which the effects of traversing objects convective accelerations should not be disregarded for velocities larger than this limit. The significance of moving load inertia and velocity on the dynamics of various beam structures has been also focused by other researchers. Hasheminejad and Rafsanjani [11] studied the action of an arbitrary moving load on the transient elastodynamic response of a thick simply supported beam. Rajabi et al. [12] investigated the influences of a moving inertial load on the dynamic behavior of functionally graded Euler–Bernoulli beams with simple end conditions. Pirmoradian et al. [13] analyzed the instability and resonance of a Timoshenko beam excited by the moving masses traversing the beam, periodically. Considering a vehicle as a traveling mass on the beams, Wang and Ko [14] assessed the vehicle-beam coupling effects when the vehicle passes the beam with variable speeds. Further researches have aimed at appraising the design dynamic parameters of single-/multi-span beams with various boundary conditions, by Kiani et al. [15,16].

It is strongly approved by the specialists and bridge engineers that the moving mass model outputs are distinctly diverse from those obtained by employing a moving force, depending on the effective parameters of the problems. In some recent researches, it has been highlighted that the moving mass simulation could be reasonably employed capturing the dynamics of a real parameter bridge [8,17]. As mentioned earlier, for heavy loads moving at high velocities, the load inertia dominates the analysis results; consequently, the moving mass appears to be a reasonable model in most of the cases. However, unfortunately, the moving mass simulation demands notable computational efforts, even in case of recently proposed optimized methods [17,18]; as a consequence of the increased complexity in the governing differential equations of motion, being time consuming in the numerical experiments, such analysis would not be favorable for the engineering practitioners. On the other hand, in all the articles mentioned, it has not been suggested any strategy/solution to overcome this issue. In fact, all these researches have only accounted for studying the importance of moving load inertia and exploring the dynamics of beams by providing the beam design parameters' spectra.

In this paper, practitioners are provided with an effortless and highly simplified direct prediction of design parameters when inertial interactions are taken into consideration. To this aim, the dynamic response of a thin beam of arbitrary boundary conditions to a moving lumped inertial object is focused. The dynamic perfor-mance of the structure is inspected in detail for a comprehensive range of velocity and inertia parameters. The voluminous computational data of the beam deformation and flexural moment are processed via regression, and the overall dynamic behavior of the base beam is ultimately represented in a remarkably reduced form. The obtained set of conversion coefficients in this regard comprises the contribution of the convective accel-eration terms. Therefore, the engineers can conveniently deal with the beam dynamic behavior in a direct and straightforward fashion. The numerical data are provided by making recourse to the characteristic orthogonal polynomials (COPs) for discretization of the spatial domain. Unlike the common proposed spatial discretiza-tion methods such as eigenfunction expansion method (EEM) [19,20], this one is very handy and rapid. Then the conversion coefficients are determined by the regression models as function of moving mass weight and velocity; afterward, the ratio of *moving mass–moving force* normalized response is achieved. Finally, after evaluating the accuracy of regression models according to goodness-of-fit statistics, the proficiency and gener-alization of the coefficients in guesstimating the inertial effects of moving loads on the beam design parameters (the maximum deflection and bending moment) are discussed.

2 Problem formulation

Let us consider a single-span Euler–Bernoulli beam of length L and uniform, rectangular cross-section, acted upon by a load $f(x, t)$ due to a mass m moving at a constant velocity v along the longitudinal direction of the beam. Let the reference frame be as reported in Fig. 1, with the origin of the x-axis placed at the left support of the beam.

To represent arbitrary end constraints, transversal and torsional springs with constants K_z and K_y are, respectively, placed at beam end cross-sections. Relevant values of constants K_z and K_y are shown in Table 1 for boundary conditions (BCs) corresponding to simply supported or pinned (P), clamped (C) and free (F) cross-sections. Needless to say, intermediate values (namely, positive finite values) of these constants can be adopted for compliant restraints.

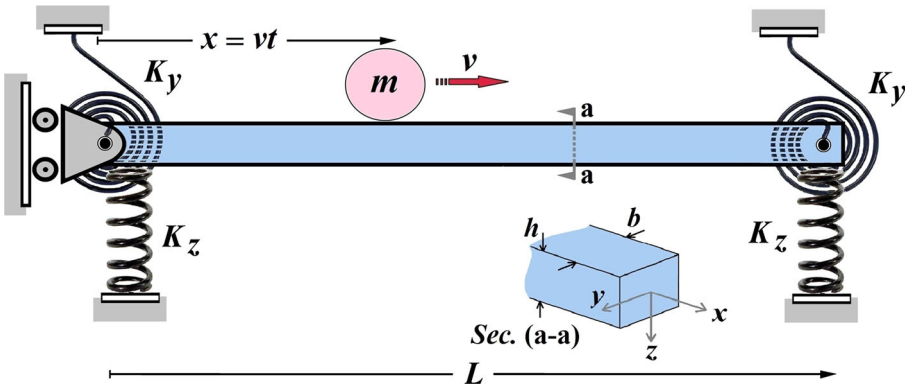

Fig. 1 Schematic of a single-span beam excited by a moving mass m

Table 1 Values of K_z and K_y for boundary conditions corresponding to pinned (P), clamped (C) and free (F) cross-sections

BCs	P	C	F
K_z	∞	∞	0
K_y	0	∞	0

Let $D(x,t)$ denote the vertical deflection of the beam, a function of the longitudinal coordinate x and of time t; the differential equation governing the elastic vibrations of an Euler–Bernoulli beam turns out to be:

$$\rho A\frac{\partial^2 D(x,t)}{\partial t^2}+EI\frac{\partial^4 D(x,t)}{\partial x^4}=f(x,t) \tag{1}$$

where ρ is the mass density of the beam material, and E is Young's modulus; $A=bh$ is the cross-sectional area, and $I=bh^3/12$ is the relevant moment of inertia (so that EI represents the flexural rigidity of the beam). In Eq. (1), material damping effects have been disregarded to slightly simplify the analysis.

If inertial effects due to the load mass are neglected, the external excitation $f(x,t)$ is given by:

$$f(x,t)=mg\delta(x-vt) \tag{2}$$

where g is the gravitational acceleration, and δ is the Dirac delta function [i.e., $\delta(x-vt)=1$ if $x=vt$, and $\delta(x-vt)=0$ if $x\neq vt$]. If inertial effects are instead accounted for within the so-called *moving mass* load case, we get (see also [21]):

$$\begin{aligned} f(x,t)&=m\left(g-\frac{\mathrm{d}^2 D_0(t)}{\mathrm{d}t^2}\right)\delta(x-vt)=m\left(g-\frac{\mathrm{d}^2 D(vt,t)}{\mathrm{d}t^2}\right)\delta(x-vt)\\ &=m\left(g-\frac{\partial^2 D}{\partial t^2}-2v\frac{\partial^2 D}{\partial x\partial t}-v^2\frac{\partial^2 D}{\partial x^2}\right)_{x=vt}\delta(x-vt) \end{aligned} \tag{3}$$

where $D_0(t)$ is the vertical displacement of the moving mass, namely $D_0(t)=D(x=vt,t)$. In Eq. (3), it has been assumed that the mass does not separate from the beam at any time throughout the analysis.

Exploiting a variable separation technique, the unknown deflection $D(x,t)$ can now be written as:

$$D(x,t)=\sum_{j=1}^{n}\varphi_j(x)A_j(t) \tag{4}$$

where $A_j(t)$ and $\varphi_j(x)$ are, respectively, the jth assumed shape function of the beam and the corresponding jth time-dependent amplitude. As for the fundamental shape function $\varphi_1(x)$ and the procedure to generate the other shape functions (up to n) to attain the required accuracy, a methodology based on COPs is provided in the "Appendix", where results are also collected for pinned–pinned (PP), clamped–clamped (CC), pinned–clamped (PC) and clamped–free (CF) end cross-sections. Substituting Eq. (4) into Eq. (1), we get:

$$\rho A\sum_{j=1}^{n}\varphi_j(x)A_{j,tt}(t)+EI\sum_{j=1}^{n}\varphi_{j,xxxx}(x)A_j(t)=m(g+\sum_{j=1}^{n}\Theta_j)\delta(x-vt) \tag{5}$$

where

$$\Theta_j = \begin{cases} 0 & \text{if moving force} \\ -\varphi_j(vt)A_{j,tt}(t) - 2v\varphi_{j,x}(vt)A_{j,t}(t) - v^2\varphi_{j,xx}(vt)A_j(t) & \text{if moving mass} \end{cases}. \tag{6}$$

Multiplying both sides of Eq. (5) by the assumed shape function $\varphi_i(x)$ and then integrating over the beam length, we arrive at:

$$\rho A \sum_{j=1}^{n} \left[\int_0^L \varphi_i(x)\varphi_j(x)\mathrm{d}x \right] A_{j,tt}(t) + EI \sum_{j=1}^{n} \left[\int_0^L \varphi_{i,xxxx}(x)\varphi_j(x)\mathrm{d}x \right] A_j(t)$$

$$= m(g + \sum_{j=1}^{n} \Theta_j)\varphi_i(vt). \tag{7}$$

The above equation could be re-written in matrix form as:

$$\mathbf{M}(t)\frac{\mathrm{d}^2}{\mathrm{d}t^2}\mathbf{A}(t) + \mathbf{C}(t)\frac{\mathrm{d}}{\mathrm{d}t}\mathbf{A}(t) + \mathbf{K}(t)\mathbf{A}(t) = \mathbf{f}(t) \tag{8}$$

where

$$[\mathbf{M}]_{ij} = \rho A \int_0^L \varphi_i(x)\varphi_j(x)\mathrm{d}x + \left[\bar{\mathbf{M}}\right]_{ij}, \tag{9}$$

$$[\mathbf{C}]_{ij} = \left[\bar{\mathbf{C}}\right]_{ij}, \tag{10}$$

$$[\mathbf{K}]_{ij} = EI \int_0^L \varphi_{i,xx}(x)\varphi_{j,xx}(x)\mathrm{d}x + \left[\bar{\mathbf{K}}\right]_{ij}, \tag{11}$$

$$[\mathbf{f}]_j = mg\varphi_j(vt), \tag{12}$$

$$[\mathbf{A}]_j = A_j(t). \tag{13}$$

The entries of matrices $[\bar{\mathbf{M}}]_{ij}$, $[\bar{\mathbf{C}}]_{ij}$ and $[\bar{\mathbf{K}}]_{ij}$ are defined for the moving force case as:

$$\left[\bar{\mathbf{M}}\right]_{ij} = \left[\bar{\mathbf{C}}\right]_{ij} = \left[\bar{\mathbf{K}}\right]_{ij} = 0 \tag{14}$$

and for the moving mass excitation as:

$$\begin{aligned} \left[\bar{\mathbf{M}}\right]_{ij} &= m\varphi_i(vt)\varphi_j(vt), \\ \left[\bar{\mathbf{C}}\right]_{ij} &= 2mv\varphi_i(vt)\varphi_{j,x}(vt), \\ \left[\bar{\mathbf{K}}\right]_{ij} &= mv^2\varphi_i(vt)\varphi_{j,xx}(vt). \end{aligned} \tag{15}$$

It should be mentioned that integral terms in $[\bar{\mathbf{K}}]_{ij}$ have been dealt with in the weak formulation accounting for the aforementioned boundary conditions.

In the literature, different numerical methods like the Newmark–Beta and Crank–Nicholson algorithms were adopted to solve the equations of motion (8) in the time domain. In this paper, the matrix exponential approach [22] has been employed; the efficiency of this method was already proved in this context, e.g., in [23,24].

3 Simplified dynamic analysis of beams excited by a moving mass

As already mentioned, in this paper, we propose a simplified analysis of beam vibrations to account for the inertial effects of a moving mass. A set of conversion coefficients is determined once and for all for the typical BCs already introduced in Sect. 2 for a single-span regular beam, so as to properly modify the response of the same beam to a moving force. According to the above discussion, this latter solution appears easier to compute and does not depend on the interaction between beam and mass inertia, which comes into play in the proposed methodology by the mentioned conversion coefficients.

On the basis of this brief discussion, the proposed procedure thus consists in the following two steps: (i) compute the dynamic response of the beam under the action of a moving mass or a moving force, with the

defined BCs; (ii) perform a nonlinear regression analysis of the effects of the moving mass on beam dynamics, having set a proper mathematical model to cover the obtained results.

For the procedure to work, the mentioned mathematical model and regression analysis have to provide results depending only on some normalization parameters accounting for the inertial properties of beam and moving mass, and for the mechanical features of the beam (basically, its geometry and elasticity). A description of the procedure and an assessment on its accuracy are reported next.

3.1 Response spectra of beam deflection

According to the analysis presented in Sect. 2, a single-span beam with a uniform, rectangular cross-section is considered. The geometrical properties of the beam are supposed to be: $L = 10$ m, $b = 0.3$m, $h = 0.6$m. The beam is assumed to be made of steel; hence, its relevant material properties are: $E = 2.1 \times 10^{11}$ Pa and $\rho = 7{,}800$ kg/m^3.

Normalization factors are introduced now according to:

$$M_{\mathrm{n}} = \frac{m}{\rho AL}, \quad V_{\mathrm{n}} = v\sqrt{\frac{\rho AL^2}{\pi^2 EI}}, \quad D_{\mathrm{n}} = \frac{D_{\mathrm{dyn}}}{D_{\mathrm{st}}}, \quad B_{\mathrm{n}} = \frac{B_{\mathrm{dyn}}}{B_{\mathrm{st}}} \tag{16}$$

where M_{n} and V_{n} are the normalized mass and velocity of the moving load, and D_{n} and B_{n} are the maximum normalized deflection of the beam and bending moment. In Eq. (16), $D_{\mathrm{dyn}}(B_{\mathrm{dyn}})$ and $D_{\mathrm{st}}(B_{\mathrm{st}})$, respectively, denote the absolute maximum dynamic deflection (bending moment) due to the moving load and the maximum static deflection (bending moment), the latter ones associated with the equivalent statically applied load. Table 2 gathers the calculated values of D_{st} and B_{st} for the considered case, at varying BCs.

The adopted geometrical and material parameters have been chosen only to provide an exemplary analysis; it was already proved in [10,15,16] that the normalization factors (16) allow describing the beam response independently of the values of all the aforementioned parameters.

The normalized spectra of beam deflection for all the considered BCs are plotted in Fig. 2 against the normalized velocity $0 < V_{\mathrm{n}} < 1$ of the load, for the two loading cases corresponding to a moving force or a moving mass featuring normalized mass M_{n} = 0.05, 0.10, 0.15, 0.20 and 0.25. It can be seen that inertial effects are enhanced if the mass and velocity of the moving load both increase. Results of Fig. 2 are in line with those provided by Kiani et al. [15].

It should be mentioned that all the spectra presented in Fig. 2 and thereafter are related to the mid-span deflection, except for the cantilever beam case whose reference point is located at the free end. Although the maximum static and dynamic beam deflections do not necessarily occur at such points, it was previously shown in [24] that the discrepancy between the spectra related to the maximum deflection point and to the mid-span point is negligible, so that reported results do not get affected.

In Fig. 2, two aspects have to be mentioned. The first one is related to the kind of hoops showing up for smaller values of V_{n}; they are basically related to the fact that the maximum beam deflection occurs at different time instants when the mass velocity varies. Hence, a single spectrum does not have to be considered as a snapshot of the structural response to the dynamic load, but instead an envelope across the whole analysis period. It may thus happen that some of the results, typically those related to the smaller V_{n} values, are linked to the forced vibrations of the beam, whereas some others are linked to the free vibrations of the beam, occurring when the moving mass has already passed along the whole length of the structure. The second aspect to point out is related to the amplitude of the normalized spectra, which may become smaller than one in some instances, see e.g., Fig. 2d. As the moving mass is always assumed to be attached to the beam, it can provide inertial forcing terms in vertical directions, sometimes acting against the current vibrations and thereby reducing their amplitude.

In Fig. 3, results are reported in terms of the ratio between the normalized deflections of the beam caused by a moving mass or a moving force. It is shown that in some cases the two responses may differ by more than

Table 2 Values of D_{st} and B_{st} for the single-span beam with various boundary conditions

BCs	PP	CC	PC	CF
$D_{\mathrm{st}}/(mgL^3/EI)$	0.02077	0.00518	0.00906	0.33333
$B_{\mathrm{st}}/(mgL)$	0.23843	0.12827	0.18623	1

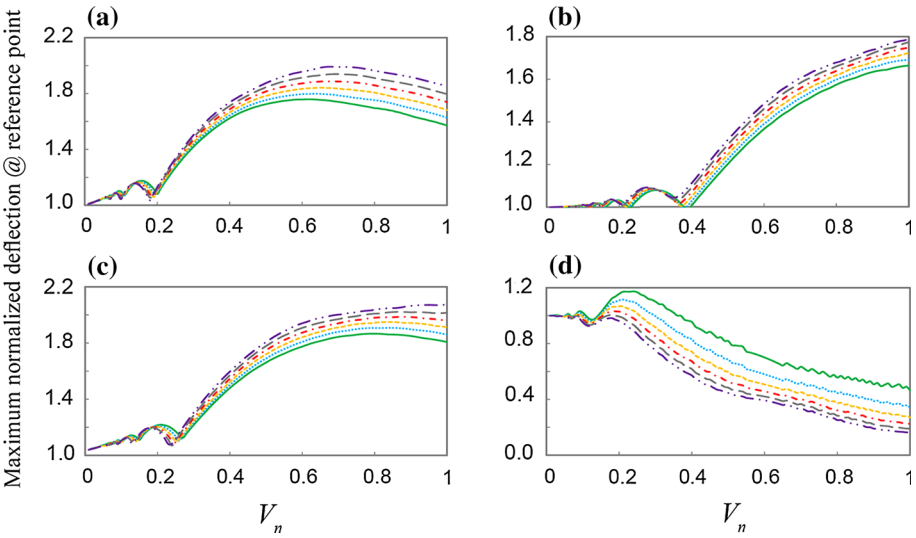

Fig. 2 Effect of the normalized mass velocity V_n on the normalized deflection spectra, at varying normalized mass (*solid line* moving force, *dotted line* $M_n = 0.05$, *dash line* $M_n = 0.10$, *dash dot line* $M_n = 0.15$, *long dash line*, $M_n = 0.20$, *dash double dot line*, $M_n = 0.25$). **a** PP, **b** CC, **c** PC, **d** CF

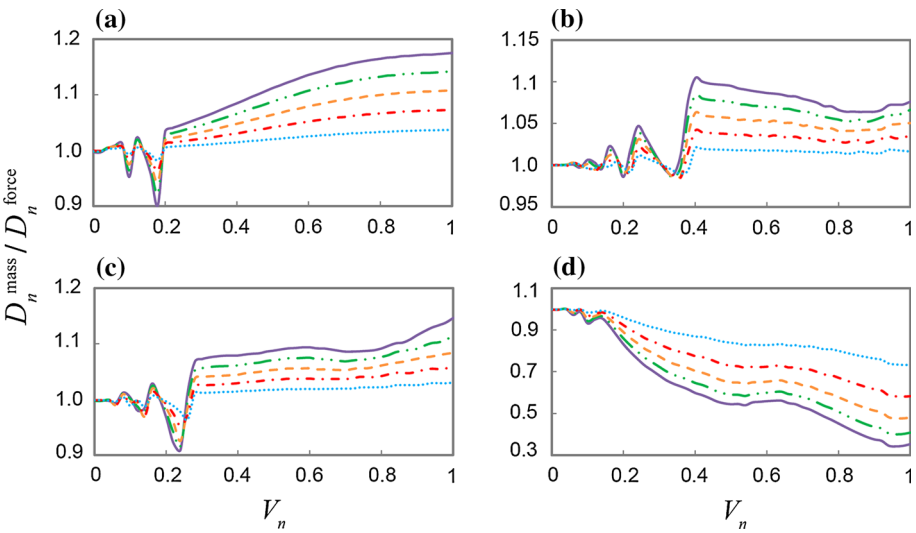

Fig. 3 Effect of the normalized mass velocity V_n on the ratio between the normalized moving mass and moving force deflection spectra, at varying normalized mass (*solid line* $M_n = 0.25$, *dash double dot line* $M_n = 0.20$, *dash line* $M_n = 0.15$, *dash dot line* $M_n = 0.10$, *dotted line* $M_n = 0.05$). **a** PP, **b** CC, **c** PC, **d** CF

15 % for PP, CC and PC boundary conditions, and even by more than 60 % for CF conditions. Such outcomes testify the need for considering the moving mass models to properly catch all the effects on the structural response. In other words, the moving force model provides some unsafe designs for the PP, CC or PC cases, or uneconomical designs for the CF case.

3.2 Regression analysis

We now move to the regression analysis of results gathered in Fig. 3.

At low values of the normalized mass velocity V_n, because of the fluctuations of the spectra and their limited variations with respect to the moving force case, evidenced by $0.90 \leq D_n^{mass} / D_n^{force} \leq 1.05$, the inertial effects of the moving mass are no further studied. Hence, the results obtained by considering the much simpler case of a moving force are assumed to always hold. According to Fig. 3, the upper limiting speed values of this

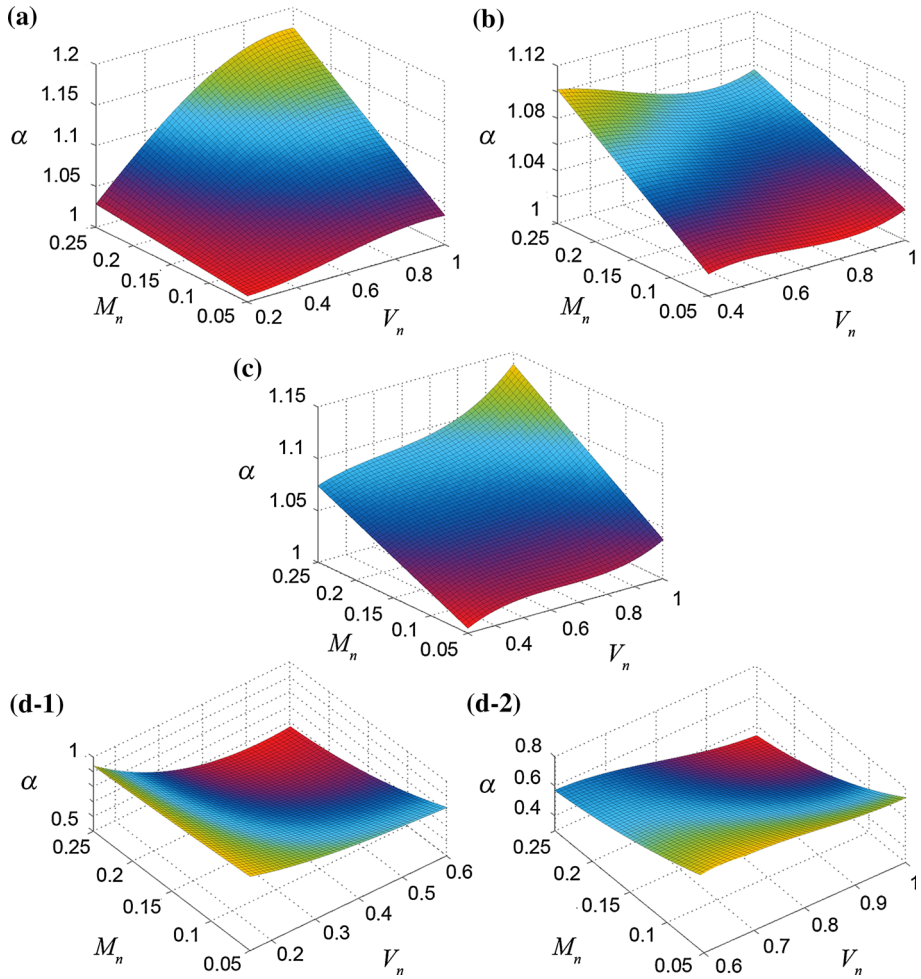

Fig. 4 Best-fit models for the moving mass effects on beam dynamics. **a** PP, **b** CC, **c** PC and **d-1**, **d-2** CF

regime are, respectively, $V_{\mathrm{n}}^{\mathrm{PP}} = 0.2$, $V_{\mathrm{n}}^{\mathrm{CC}} = 0.37$, $V_{\mathrm{n}}^{\mathrm{PC}} = 0.27$ and $V_{\mathrm{n}}^{\mathrm{CF}} = 0.15$ for the corresponding BCs. These values depend only on the physical properties of the beam, and at assigned BCs, in accordance with the normalization defined by Eq. (16), they are invariant, see also [10,15,16].

As reported in the plots of Fig. 3, the normalized spectra of $D_{\mathrm{n}}^{\mathrm{mass}}/D_{\mathrm{n}}^{\mathrm{force}}$ do not monotonically vary. Hence, to better approximate once and for all their dependence on V_{n}, the normalized mass velocity interval beyond the aforementioned limiting values may be subdivided into subintervals. For instance, to handle the outcomes relevant to the CF case, two regions are considered, according to $0.15 < V_{\mathrm{n}}^{\mathrm{CF}} \leq 0.60$ and $0.60 < V_{\mathrm{n}}^{\mathrm{CF}} < 1$. This analysis over V_{n} sub-domains does not look necessary for all the other BCs here investigated.

The regression analysis to best fit the shown spectra is now based on a polynomial function of order three in V_{n} and M_{n}, as primary variables of the model. The adopted general form of the fitting function thus reads:

$$\alpha = \frac{D_{\mathrm{n}}^{\mathrm{mass}}}{D_{\mathrm{n}}^{\mathrm{force}}} = P_{00} + P_{10}V_{\mathrm{n}} + P_{01}M_{\mathrm{n}} + P_{20}V_{\mathrm{n}}^2 + P_{11}V_{\mathrm{n}}M_{\mathrm{n}} + P_{02}M_{\mathrm{n}}^2 + P_{30}V_{\mathrm{n}}^3 + P_{21}V_{\mathrm{n}}^2M_{\mathrm{n}} + P_{12}V_{\mathrm{n}}M_{\mathrm{n}}^2 \tag{17}$$

where the constants P_{ij} (linked through indexes i and j to the power of terms in V_{n} and M_{n}, respectively) are the sought regression coefficients.

By a least-squares procedure, the results of surface fitting turn out to be as depicted in Fig. 4 for all the considered BCs. As commented here above, for CF constraint conditions, the normalized mass velocity domain beyond the threshold to effectively sense the inertial effects of the moving mass, has been subdivided into the two reported sub-domains. Figure 4d-1, d-2 accordingly shows the two relevant interpolating surfaces.

Table 3 Regression coefficients P_{ij} and goodness-of-fit assessment of the regression analysis, for all the considered boundary conditions

BCs	PP	CC	PC	CF	
V_n interval	(0.2, 1)	(0.37, 1)	(0.27, 1)	(0.15, 0.6)	(0.6,1)
Regression coefficients					
P_{00}	1.0250	0.8856	0.8946	1.098	−2.227
P_{10}	−0.1665	0.5297	0.5102	−0.742	11.86
P_{01}	−0.2242	0.6953	0.4526	1.307	1.367
P_{20}	0.2871	−0.7951	−0.7866	1.53	−14.49
P_{11}	1.8330	−0.8305	−0.5415	−12.97	−7.167
P_{02}	0	0	0	−1.164	−0.874
P_{30}	−0.1445	0.3903	0.3941	−1.183	5.778
P_{21}	−0.9142	0.3932	0.5912	10.31	1.867
P_{12}	0	0	0	10.09	7.234
Goodness of fit					
SSE	0.0001	0.0010	0.0028	0.0051	0.0064
R^2	0.9999	0.9940	0.9904	0.9985	0.9983
$\bar{R}^2$	0.9999	0.9939	0.9902	0.9985	0.9982
RMSE	0.0005	0.0018	0.0028	0.0048	0.0057

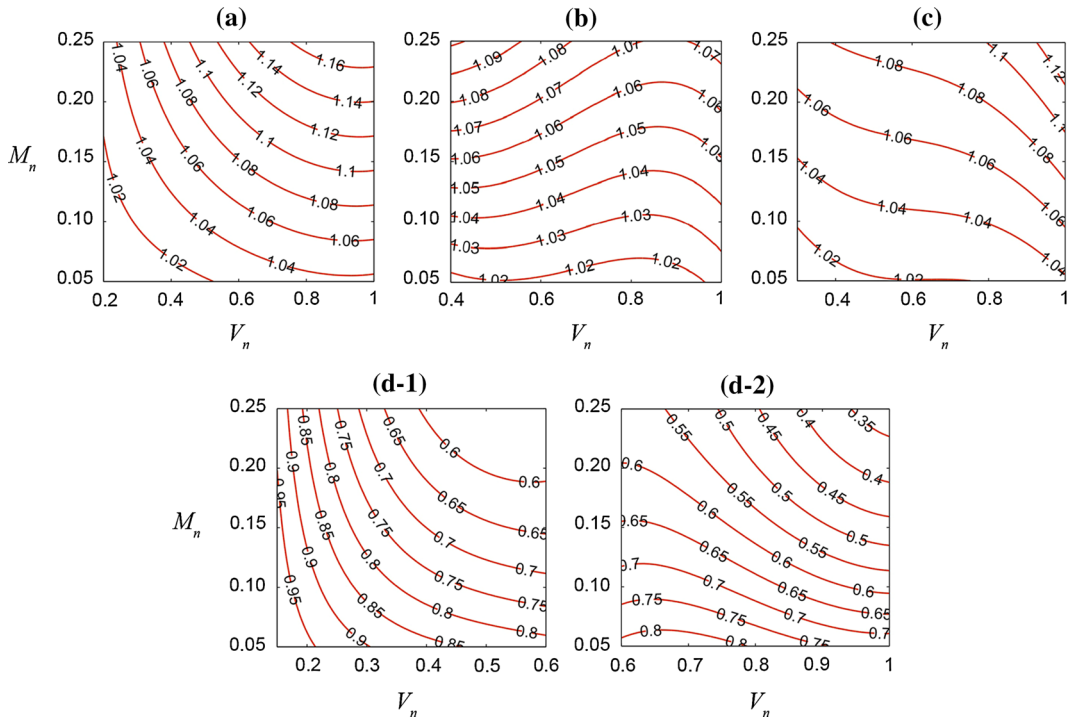

Fig. 5 Level sets of the conversion coefficient α. **a** PP, **b** CC, **c** PC, **d-1**, **d-2** CF

The regression coefficients P_{ij} for all the BCs are gathered in Table 3, along with an assessment of the resulting goodness of fit, in terms of SSE (summed square of residuals), R^2 (R square), $\bar{R}^2$ (adjusted R^2) and root-mean-squared error (RMSE) tests [25]. Table 3 and relevant Fig. 4 testify that the suggested regression model provides a very good agreement between the results, being always R^2, $\bar{R}^2 \approx 1$ and SSE, RMSE <0.01.

Results of best-fitting are finally reported in Fig. 5 as level sets of the conversion coefficient α. Such plots can be easily exploited once the values of the normalized mass M_n and velocity V_n are known, to compute the coefficient itself. Similar plots can be established for all the other quantities of interest relevant to beam dynamics, e.g., stress and strain parameters.

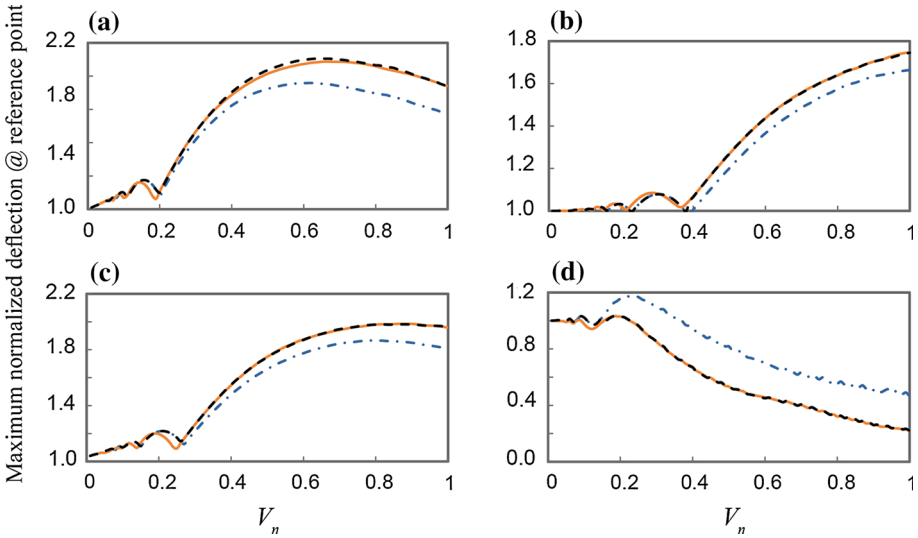

Fig. 6 Effect of the normalized mass velocity V_n on the normalized deflection spectra for **a** PP, **b** CC, **c** PC, **d** CF [*solid line* moving mass ($M_n = 0.15$), *dash dot line* moving force, *dash line* modified moving force]

Table 4 Accuracy of the estimated maximum normalized bending moment (B_n), for the beam excited by a moving mass featuring $M_n = 0.20$

BCs	V_n	B_n			
		Moving force	Moving mass	Modified moving force	Difference (%)
PP	0.1	1.04699	1.04781	1.04700	0.08
	0.5	1.52613	1.66873	1.66076	0.48
	1.0	1.41887	1.62145	1.61754	0.24
CC	0.1	1.07310	1.07344	1.07310	0.03
	0.5	1.29659	1.39545	1.39530	0.01
	1.0	2.69147	2.86292	2.85861	0.15
PC	0.1	1.21991	1.22893	1.21992	0.74
	0.5	1.85788	1.98394	1.98467	0.04
	1.0	2.59418	2.87543	2.88671	0.39
CF	0.1	1.31188	1.32352	1.31189	0.89
	0.5	1.16248	0.69049	0.69373	0.47
	1.0	0.82417	0.32033	0.32044	0.03

3.3 Accuracy of the fitting procedure

To assess the capability of the regression analysis of Sect. 3.2 to catch the inertial effects of a moving mass on beam dynamics, the beam is now assumed to be acted by a moving mass featuring $M_n = 0.15$. The maximum normalized deflection of the beam with the BCs already considered before is shown in Fig. 6 against the normalized velocity of the mass.

By comparing the spectra computed according to the procedure of Sect. 2 and linked to the moving mass and moving force cases, with the related spectra obtained by modifying the moving force ones by the conversion coefficients of Table 3, the performance of the offered procedure can be neatly evidenced. Accordingly, by first conducting a simple and rapid dynamic analysis of the beam excited by a moving force and then employing the conversion coefficients, inertial effects of the moving mass can be appropriately accounted for.

4 Generalization of the conversion coefficients

As already pointed out, conversion coefficients can be established once and for all and then adopted not only to predict the spectra of maximum deflection, but also e.g., the spectra of maximum bending moment. Relevant results are collected in Table 4 for a mass $M_n = 0.20$ moving with normalized velocity values $V_n = 0.1$, 0.5 and 1.0. Outcomes are once again reported for all the considered BCs, in terms of values corresponding to

the full solution given by the moving force and moving mass, and by converting the moving force case via the coefficients still obtained with the regression analysis. The relative difference between the original and corrected solutions, shown in the rightmost column as being smaller than 1 %, testifies the attained accuracy of the solution.

For ease of analysis, similar to what was done for the lateral deflection of the beam, the reference point where the maximum normalized bending moment has been set a priori is located at the mid-span for the PP case, and at the clamped end for the CC, PC and CF cases.

5 Conclusions

In this paper, conversion coefficients have been computed to automatically obtain the dynamic solution of a single-span slender beam excited by a moving mass from the corresponding solution linked to a moving force. As reported, in the former case, the interaction between the beam motion and the mass inertia is more difficult to handle computationally: hence, the proposed methodology behind the computed coefficients is expected to allow time savings in the analysis of beam dynamics.

A beam with different end (boundary) conditions has been considered, and a handy semi-analytical method has been discussed to compute its dynamics, employing COPs to approximate beam deflection. By an exemplary case, the maximum deflection induced by a moving mass or a moving force has been computed, and the proposed regression analysis has been run. The regression functions have been assumed as cubic polynomial ones of order three, with a reported high goodness of fit independently of the mass and velocity of the loading system. The major feature of the obtained conversion coefficients is that they do not depend on the problem at hand, since mass, mass velocity, and beam deflection or bending moment have been all appropriately normalized, so that the coefficients here provided are always valid.

The proposed model thus leads to a satisfactory solution to estimate the inertial effects of moving loads on beam-like structures. It has also been shown that the obtained conversion coefficients have a remarkable accuracy also to transform other design parameters linked to a moving force into those related to a moving mass.

Finally, it looks worth pointing out that the proposed method can be routinely used to post-process results of analyses of beam structures carried out with, e.g., commercial software, without any external subroutine necessary to properly account for the aforementioned effects of moving masses.

Acknowledgments S.M. wishes to acknowledge a partial financial support from Fondazione Cariplo by Project Safer Helmets.

Appendix

Exploiting a procedure based on the COPs in the Rayleigh–Ritz method, the shape functions for the single-span beam can be computed for any boundary condition, see e.g., [26,27]. In this context, the first shape function $\varphi_1(x)$ is assumed as a polynomial function of order four, to satisfy the natural and geometrical BCs [28]. Accordingly:

$$\varphi_1(x) = \frac{3}{\sqrt{L}} \begin{cases} \frac{\sqrt{2{,}170}}{31}\left[\left(\frac{x}{L}\right) - 2\left(\frac{x}{L}\right)^3 + \left(\frac{x}{L}\right)^4\right] & \text{if PP} \\ \sqrt{70}\left[\left(\frac{x}{L}\right)^2 - 2\left(\frac{x}{L}\right)^3 + \left(\frac{x}{L}\right)^4\right] & \text{if CC} \\ \frac{\sqrt{1{,}330}}{19}\left[\left(\frac{x}{L}\right) - 3\left(\frac{x}{L}\right)^3 + 2\left(\frac{x}{L}\right)^4\right] & \text{if PC} \\ \frac{\sqrt{130}}{52}\left[6\left(\frac{x}{L}\right)^2 - 4\left(\frac{x}{L}\right)^3 + \left(\frac{x}{L}\right)^4\right] & \text{if CF} \end{cases} . \tag{A1}$$

Additional shape functions to increase the accuracy of the solution are obtained by employing the Gram–Schmidt procedure, leading to [27,28]:

$$\varphi_2(x) = (x - P_2)\varphi_1(x), \tag{A2}$$

$$\varphi_n(x) = (x - P_n)\varphi_{n-1}(x) - Q_n\varphi_{n-2}(x); \quad n = 3, 4, 5, \ldots \tag{A3}$$

where

$$P_n = \frac{\int_0^L x\left[\varphi_{n-1}(x)\right]^2 W(x)\mathrm{d}x}{\int_0^L \left[\varphi_{n-1}(x)\right]^2 W(x)\mathrm{d}x}; \quad n = 2, 3, 4, \ldots, \tag{A4}$$

$$Q_n = \frac{\int_0^L x\varphi_{n-1}(x)\varphi_{n-2}(x)W(x)\mathrm{d}x}{\int_0^L \left[\varphi_{n-2}(x)\right]^2 W(x)\mathrm{d}x}; \quad n = 3, 4, 5, \ldots \tag{A5}$$

In the equations above, $W(x)$ is a weight function which is taken unit in this study. The polynomial functions thus obtained are always orthogonal; i.e.,:

$$\int_0^L \varphi_a(x)\varphi_b(x)W(x)\mathrm{d}x \begin{cases} = 0 & \text{if } a \neq b \\ \neq 0 & \text{if } a = b \end{cases}. \tag{A6}$$

References

1. Steele, C.: The finite beam with a moving load. J. Appl. Mech. **34**, 111–118 (1967)
2. Knowles, J.: On the dynamic response of a beam to a randomly moving load. J. Appl. Mech. **35**, 1–6 (1968)
3. Sridharan, N., Mallik, A.: Numerical analysis of vibration of beams subjected to moving loads. J. Sound Vib. **65**, 147–150 (1979)
4. Hayashikawa, T., Watanabe, N.: Dynamic behavior of continuous beams with moving loads. J. Eng. Mech. Div. **107**, 229–246 (1981)
5. Jaiswal, O.R., Iyengar, R.N.: Dynamic response of a beam on elastic foundation of finite depth under a moving force. Acta Mech. **96**, 67–83 (1993)
6. Akin, J.E., Mofid, M.: Numerical solution for response of beams with moving mass. J. Struct. Eng. **115**, 120–131 (1989)
7. Rao, G.V.: Linear dynamics of an elastic beam under moving loads. ASME J. Vib. Acoust. **122**, 281–289 (2000)
8. Michaltsos, G.T., Kounadis, A.N.: The effects of centripetal and Coriolis forces on the dynamic response of light bridges under moving loads. J. Vib. Control **7**, 315–326 (2001)
9. Ichikawa, M., Miyakawa, Y., Matsuda, A.: Vibration analysis of the continuous beam subjected to a moving mass. J. Sound Vib. **230**, 493–506 (2000)
10. Nikkhoo, A., Rofooei, F., Shadnam, M.: Dynamic behavior and modal control of beams under moving mass. J. Sound Vib. **306**, 712–724 (2007)
11. Hasheminejad, S.M., Rafsanjani, A.: Two-dimensional elasticity solution for transient response of simply supported beams under moving loads. Acta Mech. **217**, 205–218 (2011)
12. Rajabi, K., Kargarnovin, M.H., Gharini, M.: Dynamic analysis of a functionally graded simply supported Euler–Bernoulli beam subjected to a moving oscillator. Acta Mech. **224**, 425–446 (2013)
13. Pirmoradian, M., Keshmiri, M., Karimpour, H.: On the parametric excitation of a Timoshenko beam due to intermittent passage of moving masses: instability and resonance analysis. Acta Mech. (2014). doi:10.1007/s00707-014-1240-z
14. Wang, Y.M., Ko, M.Y.: The interaction dynamics of a vehicle traveling along a simply supported beam under variable velocity condition. Acta Mech. **225**, 3601–3616 (2014)
15. Kiani, K., Nikkhoo, A., Mehri, B.: Prediction capabilities of classical and shear deformable beam models excited by a moving mass. J. Sound Vib. **320**, 632–648 (2009)
16. Kiani, K., Nikkhoo, A., Mehri, B.: Assessing dynamic response of multispan viscoelastic thin beams under a moving mass via generalized moving least square method. Acta Mech. Sin. **26**, 721–733 (2010)
17. Ebrahimzadeh Hassanabadi, M., Vaseghi Amiri, J., Davoodi, M.R.: On the vibration of a thin rectangular plate carrying a moving oscillator. Sci. Iran. Trans. A Civ. Eng. **21**, 284–294 (2014)
18. Ebrahimzadeh Hassanabadi, M., Attari, N.K.A., Nikkhoo A., Baranadan, M.: An optimum modal superposition approach in the computation of moving mass induced vibrations of a distributed parameter system. Proc. Inst. Mech. Eng. Part C: J. Mech. Eng. Sci. (2014). doi:10.1177/0954406214542968
19. Ouyang, H.: Moving-load dynamic problems: a tutorial (with a brief overview). Mech. Syst. Signal Process. **25**, 2039–2060 (2011)
20. Bajer, C.I., Dyniewicz, B.: Numerical Analysis of Vibrations of Structures Under Moving Inertial Load. Springer, Berlin (2012)
21. Frýba, L.: Vibration of Solids and Structures Under Moving Loads. Thomas Telford, London (1999)
22. Brogan, W.L.: Modern Control Theory. Prentice-Hall, Upper Saddle River (1991)
23. Nikkhoo, A., Rofooei, F.R.: Parametric study of the dynamic response of thin rectangular plates traversed by a moving mass. Acta Mech. **223**, 15–27 (2012)
24. Nikkhoo, A.: Investigating the behavior of smart thin beams with piezoelectric actuators under dynamic loads. Mech. Syst. Signal Process. **45**, 513–530 (2014)
25. http://web.maths.unsw.edu.au/~adelle/Garvan/Assays/GoodnessOfFit.html. (Accessed 1 Oct 2014)
26. Bhat, R.: Natural frequencies of rectangular plates using characteristic orthogonal polynomials in Rayleigh–Ritz method. J. Sound Vib. **102**, 493–499 (1985)
27. Chakraverty, S.: Vibration of Plates. CRC Press, Boca Raton (2010)
28. Nikkhoo, A., Farazandeh, A., Ebrahimzadeh Hassanabadi, M.: On the computation of moving mass/beam interaction utilizing a semi-analytical method. J. Braz. Soc. Mech. Sci. Eng. (2014). doi:10.1007/s40430-014-0277-1